veterinary sciences

MDPI

Article

Isolation, Multidrug Resistance Profiling, and Whole-Genome Analysis of *Escherichia coli* from Foals with Diarrhea in Ili, Xinjiang, China

Xuanpan Ding [1], Xiuzhi Liu [1], Tingyang Wu [1], Yuhui Ma [2], Yuan Zhao [1,*] and Honggang Fan [1,*]

[1] Heilongjiang Key Laboratory for Laboratory Animals and Comparative Medicine, College of Veterinary Medicine, Northeast Agricultural University, Harbin 150030, China; a1910225288@163.com (X.D.)
[2] Zhaosu County Western Regions Horse Industry Co., Ltd., Yining 835000, China
* Correspondence: 16645266261@163.com (Y.Z.); fanhonggang2002@163.com (H.F.)

Simple Summary

Diarrhea in young horses is a serious problem for breeders, and the bacteria that cause it are becoming increasingly difficult to treat with medicines. We studied fecal samples from diarrheic foals in the Ili region of China to find out how widespread these resistant bacteria are and what makes them harmful. More than half of the isolated bacteria could resist several types of medicines at the same time. We then performed a detailed genetic analysis of one representative strain. This strain contained a large number of genes related to drug resistance and disease-causing ability, and it was highly capable of forming a protective slime layer and causing severe illness in laboratory mice. Our findings show that horses can carry and potentially pass on dangerous bacteria to other animals and humans. This highlights the need for better monitoring of resistance in horses and for more careful use of medicines in veterinary care to protect both animal and human health.

Abstract

Background: *Escherichia coli* (*E. coli*) is a leading cause of diarrhea in neonatal foals, and the emergence of multidrug-resistant (MDR) strains poses a growing threat to equine health and public health. However, antimicrobial resistance surveillance in equine *E. coli* remains limited, particularly in Xinjiang, a major horse-breeding region in China. Objective: To isolate and identify *E. coli* from diarrheic foals in Ili, Xinjiang, characterize their antimicrobial resistance phenotypes, and perform whole-genome sequencing on a representative MDR strain to elucidate its resistance mechanisms, virulence potential, and transmission risk. Methods: A total of 78 fecal samples were collected from diarrheic foals between May 2025 and June 2026. Isolates were identified by culture, Gram staining, and 16S rRNA gene sequencing. The antibiotic susceptibility of the isolated bacteria was determined using the Kirby–Bauer diffusion method. A representative MDR strain, YN1, was subjected to PacBio and Illumina whole-genome sequencing. Resistance genes, virulence factors, and mobile genetic elements were annotated using CARD, VFDB, and CAZy databases, and key findings were validated by PCR, biofilm assays, and a murine pathogenicity model. Results: A total of 58 *E. coli* strains were isolated (isolation rate, 74.36%), with the highest rate (83.33%) in foals aged 0–3 months. MDR was detected in 63.79% of isolates. Strain YN1 possessed a 4,951,512 bp chromosome and a 130,938 bp plasmid (cgMLST type cgST134023), encoding 107 predicted resistance genes and 204 predicted virulence determinants. Resistance was mediated primarily by chromosomally encoded efflux systems, supplemented by the plasmid-borne *blaTEM*. YN1 formed strong biofilms and caused lethal infection in mice within an average of 16 h, with severe hemorrhage and congestion in the lungs, spleen,

Check for updates

Academic Editor: Kun Li

Received: 21 October 2026
Revised: 14 November 2026
Accepted: 15 November 2026
Published: 17 November 2026

Copyright: © 2026 by the authors. Licensee MDPI, Basel, Switzerland. This article is an open access article distributed under the terms and conditions of the Creative Commons Attribution (CC BY) license.

and liver. Conclusion: MDR *E. coli* is highly prevalent among diarrheic foals in Ili, Xinjiang. The representative strain YN1 carried extensive resistance and virulence determinants and exhibited strong pathogenicity, highlighting the need for strengthened antimicrobial resistance surveillance and rational antimicrobial use in equine practice.

Keywords: *Escherichia coli*; horse; antibiotic resistance; infection; virulence factors; One Health

1. Introduction

The intensifying global crisis of antimicrobial resistance (AMR) has profoundly transformed the clinical and ecological framework of veterinary medicine [1,2]. However, its extent within equine populations remains insufficiently characterized. Equines occupy a unique position at the human–animal interface, functioning simultaneously as sports partners, companion animals, and agricultural resources. This proximity facilitates bidirectional transmission pathways for resistant bacteria, challenging traditional species boundaries and highlighting the critical need for a One Health approach to equine AMR surveillance [3,4].

Escherichia coli (*E. coli*) serves as both a commensal indicator organism and a versatile pathogen, capable of inducing severe enteric and extraintestinal infections in neonatal foals [5]. Contemporary evidence presents a more concerning scenario: MDR *E. coli* is now prevalent within equine populations, with extended-spectrum beta-lactamase (ESBL)-producing strains colonizing up to 84% of equines in certain clinical settings and showing phenotypic resistance to three or more antimicrobial classes in over 90% of isolates [6]. Despite this significant burden, surveillance of equine *E. coli* has lagged considerably behind that of food-producing animals, resulting in critical gaps in our understanding of resistance mechanisms, transmission dynamics, and zoonotic risk.

The clinical significance of MDR *E. coli* in foals is exacerbated by the distinct ecological pressures characteristic of equine environments. In contrast to intensively housed livestock, equines are managed in a manner that facilitates both close human interaction and significant environmental contamination via fecal shedding [7]. Recent genomic studies conducted in Xinjiang, one of China's major horse-breeding regions, have begun to elucidate the molecular mechanisms underlying resistance in this context. Investigations of dairy farm environments in the region have identified MDR *E. coli* strains possessing a variety of efflux-associated genes, secretion systems, and biofilm-associated determinants, with some strains being classified as potential human pathogens [8]. These findings indicate that the agro-ecological context of Xinjiang may promote the accumulation of resistance determinants through mechanisms that are not yet fully understood.

Whole-genome sequencing (WGS) has become an essential methodology for elucidating the genetic framework underlying resistance and virulence in bacterial pathogens. It facilitates the accurate identification of resistance genes, virulence factors, mobile genetic elements, and their localization on chromosomes or plasmids [9,10]. In the context of equine *E. coli*, WGS has demonstrated that clonal dissemination, plasmid-mediated horizontal gene transfer, and chromosomal mutations collectively contribute to the development of resistance phenotypes. Nevertheless, such comprehensive analyses have been infrequently conducted on diarrheic foals in China, and high-quality reference genomes for MDR equine E. coli from this region remain scarce. Establishing such reference genomes is a prerequisite for future comparative studies aimed at identifying host-associated genomic features.

This study aims to address existing knowledge gaps by conducting a comprehensive phenotypic and genomic analysis of *E. coli* strains isolated from foals with diarrhea in the Ili region of Xinjiang. To investigate whether MDR *E. coli* from this region possesses transfer-

able resistance and virulence determinants, as well as high pathogenicity and the potential for cross-species transmission, we generated a high-quality, representative reference genome of an MDR strain and examined its resistance profile, virulence, and repertoire of mobile genetic elements. To evaluate this hypothesis, we analyzed the antimicrobial susceptibility profiles of the collected isolates and conducted PacBio and Illumina whole-genome sequencing on a representative MDR strain (YN1). Key genomic findings were further validated through PCR, biofilm assays, and a murine pathogenicity model. By linking phenotypic resistance patterns to their genomic bases, this research aims to provide a mechanistic foundation for antimicrobial stewardship and surveillance strategies, recognizing equines as sentinel hosts within the One Health framework.

2. Materials and Methods

2.1. Sample Collection and Test Materials

From May 2025 to June 2026, fecal samples were collected from foals with diarrhea in Yining City (81–82° E, 43–44° N), for bacterial isolation and identification. Prior to sample collection, the foals were restrained, and their perianal regions were disinfected using 0.1% benzalkonium bromide. Sterile swabs were then employed to collect fecal samples directly from the rectum. Fecal samples were also collected from healthy foals in the same herds to serve as controls. Animal experiments were conducted using six-week-old female specific-pathogen-free (SPF) Kunming mice weighing 18–20 g, (Harbin, China). Bacterial isolation, amplification, and antibiotic susceptibility testing were carried out using nutrient broth, Mueller–Hinton broth, MacConkey agar, alongside other reagents and materials supplied by Servicebio (Wuhan, China). An incubator (Aolei, Jinan, China), a bacterial genome extraction kit (Jingmei Biotechnology, Nanjing, China), a PCR amplifier (Pulton Technology, Houston, TX, USA), and a gel imaging system (APExBIO, Houston, TX, USA), among other equipment, were used for genomic analysis and phenotypic validation.

2.2. Pathogen Isolation and Detection

2.2.1. Bacterial Isolation

The collected fecal swabs were inoculated into Luria–Bertani (LB) broth and incubated at 37 °C with agitation for 6 to 8 h to promote bacterial proliferation. Subsequently, an inoculation loop was used to transfer the enriched culture onto MacConkey agar plates, which were then incubated at 37 °C for 18 to 24 h. MacConkey agar is formulated with bile salts and crystal violet, which selectively inhibit the growth of Gram-positive bacteria. *E. coli* ferments lactose, resulting in acid production that causes the colonies to appear pink or red. Colonies exhibiting typical *E. coli* morphology (pink, round, smooth, with well-defined edges) were selected from the MacConkey agar plate and streaked onto an eosin-methylene blue (EMB) agar plate for further purification, followed by incubation at 37 °C for an additional 18 to 24 h. On EMB agar, *E. coli* typically forms black colonies with a metallic sheen. A single representative colony was isolated and inoculated onto a nutrient agar slant to establish a pure culture, which was then reserved for further analysis.

2.2.2. Bacterial Identification

Gram staining and microscopic examination: A smear was prepared from a purified single colony; after Gram staining, the morphology and staining characteristics of the bacteria were observed under an oil immersion microscope. *E. coli* is a Gram-negative short rod, arranged singly or in pairs, with dimensions of approximately 0.5 × 1–3 μm.

16S rRNA Gene Sequence Analysis: A single purified colony was selected, and total bacterial DNA was extracted according to the instructions of the bacterial genomic

DNA extraction kit. PCR amplification was performed using universal bacterial 16S rRNA primers with the following sequences: F (5′-AGAGTTTGATCMTGGCTCAG-3′) and R (5′-GGTTACCTTGTTACGACTT-3′). After detecting the amplification products via 1% agarose gel electrophoresis, they were sent to Shengong Bioengineering (Shanghai) Co., Ltd. for sequencing. The sequencing results were compared with known sequences in the NCBI GenBank database using BLAST (https://www.ncbi.nlm.nih.gov/, accessed on 20 October 2026); those with ≥99% homology were identified as the corresponding bacterial species.

2.2.3. Antibiotic Susceptibility Testing

Refer to our previous research [11]. The Kirby–Bauer disk diffusion method was employed to assess the susceptibility of isolated strains to a range of commonly utilized clinical antibiotics. The antibiotics selected for this study encompassed six major classes: β-lactams, aminoglycosides, carbapenems, tetracyclines, fluoroquinolones, and sulfonamides. The procedure was conducted as follows: A purified single colony was inoculated into LB broth and incubated with shaking at 37 °C for 4–6 h until reaching the logarithmic growth phase. The bacterial suspension was then adjusted to a concentration of 0.5 McFarland units (approximately 1.5×10^8 CFU/mL) using sterile saline. A sterile cotton swab was immersed in the bacterial suspension and used to evenly distribute the bacteria over the surface of a Mueller–Hinton agar plate. The plate was allowed to dry slightly at ambient temperature for 3 to 5 min. Subsequently, using sterile forceps, an antibiotic disc was carefully placed in direct contact with the agar surface. The plate was then incubated in an inverted position at 37 °C for 18 to 24 h. Following incubation, the diameter of the inhibition zone was measured using a Vernier caliper. The strain's response to each antibiotic was classified as susceptible, intermediate, or resistant based on the interpretation criteria outlined in the 2023 edition of the CLSI M100 document published by the Clinical and Laboratory Standards Institute [12]. According to these guidelines, multidrug resistance is characterized by the absence of susceptibility (i.e., resistance or intermediate susceptibility) of an isolated strain to at least one drug from three or more classes of antibiotics. In this study, the resistance profiles of the isolated strains to six major classes of antibiotics were examined, and strains exhibiting resistance to three or more classes were categorized as multidrug-resistant.

2.3. Whole-Genome Sequencing of Representative Strains

Following antibiotic susceptibility testing, a new multidrug-resistant *E. coli* strain (YN1) was isolated for comprehensive whole-genome sequencing analysis. The activated YN1 strain was inoculated into LB broth and incubated with shaking at 37 °C until the logarithmic growth phase was reached. An appropriate volume of the bacterial culture was centrifuged at 4000× *g* for 10 min at 4 °C to collect the bacterial pellet, and the supernatant was discarded. Total DNA was extracted from the YN1 strain according to the instructions for the bacterial genomic DNA extraction kit. The integrity of the extracted DNA was verified by 1% agarose gel electrophoresis, and its concentration and purity were assessed using an ultramicro spectrophotometer (OD260/280 between 1.8 and 2.0, and OD260/230 greater than 2.0).

DNA samples meeting the quality requirements were sent to Shanghai Meiji Technology Co., Ltd. (Shanghai, China) for whole-genome sequencing. A hybrid sequencing strategy combining second- and third-generation platforms was employed. Library construction and quality assessment were performed using the PacBio and Illumina platforms. After confirming library quality, sequencing was conducted using the PacBio Sequel and Illumina NovaSeq PE150 systems. The PacBio platform generated ~150× coverage of long reads (average read length ~10 kb), and the Illumina platform generated ~100× coverage of

paired-end short reads (2 × 150 bp). For genome assembly, the PacBio long reads were first de novo assembled using SOAPdenovo2 software (v2.04) (http://soap.genomics.org.cn/, accessed on 20 October 2026). The resulting contigs were then polished and corrected using Illumina short reads via the Pilon software (v1.23) to obtain high-quality, complete bacterial genome sequences.

2.4. Bioinformatics Analysis

Genomic coding sequences (CDS) were identified using Glimmer, GeneMarkS, and Prodigal, with Prodigal applied for chromosomal genomes and GeneMarkS for plasmid genomes. tRNA prediction was performed using tRNAscan-SE v2.0, while rRNA identification utilized Barrnap to determine species, location, and sequence data. Functional annotation of coding genes was conducted via protein sequence alignment against EggNOG, Gene Ontology (GO), and KEGG databases. In addition, circular genome maps for individual samples were generated using the CGview software (JavaScript version 3.1).

2.5. Analysis of Virulence and Resistance Genes

The YN1 genome was systematically aligned with the Comprehensive Antibiotic Resistance Database (CARD), the Antibacterial Biocide and Metal Resistance Genes Database, and the Virulence Factor Database (VFDB, version 2.0), employing stringent criteria (E-value $< 1 \times 10^{-5}$, coverage $> 80\%$) to identify high-confidence resistance and virulence genes [13,14]. The resistance genes identified were categorized based on their encoded resistance mechanisms, which include antibiotic-inactivating enzymes, efflux pumps, target-modifying proteins, and target-protecting proteins. Similarly, the virulence genes were classified according to their biological functions, encompassing adhesion factors, toxins, secretion system components, immunomodulators, motility-related factors, and nutrient metabolism-related factors. Furthermore, protein interaction networks of resistance genes and virulence factors in YN1 were constructed utilizing the STRING database (https://cn.string-db.org/, accessed on 20 October 2026) and Cytoscape tool (Version 3.7), with *E. coli K12 MG1655* serving as the reference. The minimum protein interaction score was set to a high confidence threshold of 0.700.

2.6. Metabolic System Analysis

The analysis of metabolic systems encompassed the annotation of carbohydrate-active enzymes and the examination of gene clusters associated with the synthesis of secondary metabolites. Carbohydrate-active enzymes are categorized into six distinct protein families: glycosidases (GHs), glycosyltransferases (GTs), polysaccharide lyases (PLs), carbohydrate esterases (CEs), carbohydrate-binding modules (CBMs), and auxiliary oxidoreductases (AAs). This classification is predicated on the similarity of amino acid sequences within protein domains. The annotation analysis was conducted utilizing the Carbohydrate-Active Enzymes database [15]. Genes with high confidence were identified through the screening of alignment results, employing a coverage threshold of greater than 80%.

2.7. Transference Analysis

To assess the zoonotic risk of drug-resistance genes, the YN1 genome was analyzed for mobile genetic elements (MGEs) like insertion sequences, transposons, and integrons using MobileElementFinder and ISfinder. Plasmid replicon types and MLST were identified via PlasmidFinder and pMLST to evaluate similarity to known conjugative plasmids. Resistance gene-carrying plasmids were compared to human clinical isolate plasmids using BLASTn against the NCBI Nucleotide Database.

2.8. PCR Confirmation of Selected Resistance and Virulence Genes

For PCR confirmation, genes predicted to be clinically relevant in the genome-wide analysis were selected. The *E. coli* reference strain ATCC 25922 served as the negative control group for target genes not expected in this standard strain. Genomic DNA was extracted from strain YN1 and used as the template. The PCR mix included 20 µL of 2× Taq Master Mix, 16 µL ddH_2O, 1 µL each of forward and reverse primers, and 2 µL template DNA. The thermal cycling conditions were 95 °C for 3 min, 34 cycles of 95 °C for 30 s, 58 °C for 30 s, and 72 °C for 1 min, followed by a final extension at 72 °C for 5 min. PCR products were analyzed using 1% agarose gel electrophoresis. (Details of primers for virulence and drug resistance genes are provided in the Supplementary Materials).

2.9. Biofilm Formation Test

In this study, staining techniques were employed to perform a comprehensive analysis of biofilm formation by the bacterial strain under investigation [16]. Ten microliters of log-phase bacterial culture were added to 190 µL of nutrient broth and incubated at 37 °C for 24 h. After incubation, wells were washed thrice with PBS (pH 7.2–7.4), dried, and stained with 1% crystal violet for 20 min at 37 °C. The stain was removed, wells were washed with PBS, dried, and treated with 250 µL of 95% ethanol for 20 min at 37 °C. Absorbance at 595 nm was measured using a microplate reader. Negative controls (no bacteria) and ATCC 25922 controls were included, and biofilm formation was evaluated based on OD values.

2.10. Pathogenicity Test

All animal experiments were approved by the Animal Ethics Committee of Northeast Agricultural University (Approval No. NEAUEC202603110) and were conducted in strict accordance with the guidelines of the Institutional Animal Care and Use Committee (IACUC). Twelve mice were randomly allocated into two groups: a control group and an experimental model group, each comprising six mice. The experimental group was administered an intraperitoneal injection of 0.1 milliliters of pathogenic bacteria at a concentration of 1×10^8 CFU/mL, whereas the control group received an equivalent volume of saline solution. Following inoculation, the mice were monitored every 4 h for up to 24 h post infection. Clinical signs were recorded using a standardized evaluating behavior (lethargy, hunched posture), coat condition (piloerection) and responsiveness. Humane endpoints were strictly applied: mice exhibiting severe clinical signs (e.g., moribund state, inability to access food or water) were immediately euthanized via cervical dislocation following isoflurane anesthesia to prevent unnecessary suffering. At the 24-h observation period (or immediately upon reaching the humane endpoint), all surviving mice were euthanized, and subjected to dissection to assess gross pathological lesions. Organs were harvested, fixed in a 4% formaldehyde solution for 24 h, embedded in paraffin, and subsequently examined microscopically following hematoxylin and eosin (H&E) staining. Samples from the liver, spleen, and blood were also collected for bacterial re-isolation to confirm the cause of infection. The experimental outcomes were assessed using a double-blind methodology. For histopathological scoring, please refer to our previously published paper [17].

2.11. Treatment with Sensitive Drugs and Verification of Efficacy

Based on the results of antibiotic susceptibility testing, gentamicin was selected to treat foals with diarrhea. It was administered intravenously at a dose of 6.6 mg/kg once every 24 h for a course of 3 to 5 days, along with routine fluid therapy. The therapeutic effect was monitored by collecting blood samples from the foals before and after treatment for complete blood count (CBC) analysis; the treatment outcome was assessed based on a

comprehensive evaluation of clinical symptoms and CBC results. A total of 12 cases were treated and followed up.

2.12. Data Analysis

Statistical analyses were performed using SPSS Version 22.0. Data were analyzed using a *t*-test (between two groups) for histopathological examinations. Statistical graphs were generated using Prism (GraphPad Software, Inc., La Jolla, CA, USA). A p-value < 0.05 indicates a statistically significant difference.

3. Results

3.1. Epidemiological Investigation Findings

Between May 2025 and June 2026, a total of 78 fresh fecal samples were obtained from foals under 12 months of age exhibiting diarrhea at both large-scale horse farms and small-scale breeding operations in the Ili Prefecture of Xinjiang. Bacterial isolation and culture processes resulted in the identification of 58 suspected *E. coli* strains, corresponding to an overall isolation rate of 74.36%. Specifically, among the foals with diarrhea, 42 samples were collected from those aged 0–3 months, yielding 35 *E. coli* isolates and an isolation rate of 83.33%. For foals aged 3–6 months, 23 samples were collected, resulting in 16 isolates and an isolation rate of 69.56%. From foals aged 6–12 months, 13 samples were collected, yielding 7 isolates with an isolation rate of 53.85% (Table 1). The isolated strains exhibited pink colonies on MacConkey agar and black, metallic-appearing colonies on eosin-methylene blue agar medium. Gram staining revealed the presence of red, short rods approximately 1 µm in length. Identification of the strains as *E. coli* was confirmed through 16S rRNA gene sequencing (Figure 1B–D).

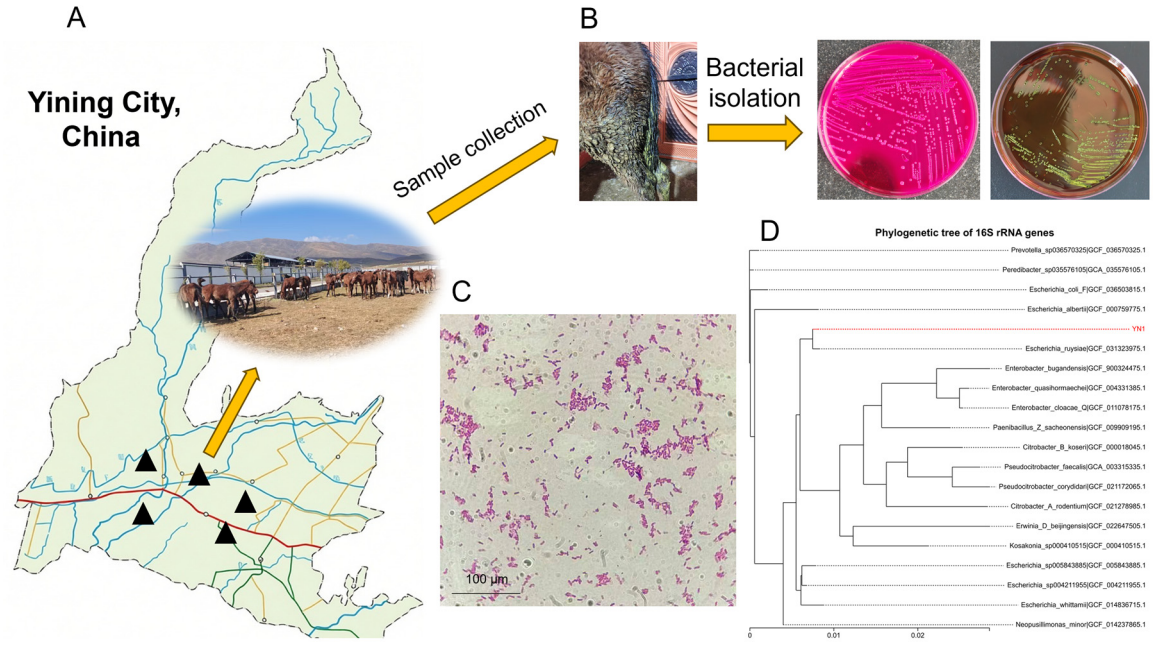

Figure 1. Isolation and identification of pathogens. (**A**) Sampling locations at the horse farm; (**B**) Morphology of *E. coli* isolated on differential media; (**C**) Microscopic findings after Gram staining; (**D**) 16S sequencing and phylogenetic tree analysis of YN1.

Table 1. Isolation of *E. coli* from faecal samples of foals of different ages with diarrhoea.

Age Group	Number of Isolates	Separation Number	Isolation Rate
0–3 months	42	35	83.33%
3–6 months	23	16	69.56%
6–12 months	13	7	53.85%

3.2. Antibiotic Susceptibility Test Results

The antimicrobial susceptibility profiles of the 58 *E. coli* isolates are presented in Table 2. All isolates exhibited susceptibility to gentamicin (100%, 58/58), followed by enrofloxacin (91.4%, 53/58), ciprofloxacin (89.7%, 52/58), tetracycline (89.7%, 52/58), imipenem (82.8%, 48/58), amikacin (81.0%, 47/58), amoxicillin (74.1%, 43/58), ampicillin (58.6%, 34/58) and sulfamonomethoxine (50%, 29/58). Intermediate resistance was most frequently observed with cefoxitin (48.3%, 28/58). According to the Clinical and Laboratory Standards Institute (CLSI) definition of MDR as non-susceptibility to at least one agent in three or more antimicrobial classes, 37 out of 58 isolates (63.79%) were classified as MDR. Among these, resistance to three classes was most prevalent (23 isolates, 39.66%), followed by resistance to two classes (16 isolates, 27.59%), four classes (9 isolates, 15.52%), five classes (4 isolates, 6.90%), and six classes (1 isolate, 1.72%). Only 5 isolates (8.62%) demonstrated resistance to a single class. These results indicate a high prevalence of MDR among equine *E. coli* in this region, with the majority of isolates resistant to multiple antimicrobial classes.

Table 2. Results of antimicrobial susceptibility testing for the isolated strains.

Categories of Antimicrobial Agents	Antimicrobial Agents	Proportion (%) of *E. coli* (n = 58)		
		Susceptible (S)	Intermediate (I)	Resistant (R)
β-lactams	Ampicillin	58.6 (34/58)	31.0 (18/58)	10.4 (6/58)
	Amoxicillin	74.1 (43/58)	0	25.9 (15/58)
	cefoxitin	18.9 (11/58)	48.3 (28/58)	32.8 (19/58)
Quinolones	Enrofloxacin	91.4 (53/58)	1.7 (1/58)	6.9 (4/58)
	Ciprofloxacin	89.7 (52/58)	0	10.3 (6/58)
Aminoglycosides	Gentamicin	100 (58/58)	0	0
	Amikacin	81.0 (47/58)	19.0 (11/58)	0
Tetracyclines	Tetracycline	89.7 (52/58)	5.2 (3/58)	5.2 (3/58)
Carbapenems	Imipenem	82.8 (48/58)	17.2 (10/58)	0
Sulphonamides	Co-trimoxazole	50 (29/58)	12.1 (7/58)	37.9 (22/58)

3.3. Results of Whole-Genome Sequencing and Cgmlst Typing of Representative Multidrug-Resistant Strains

Upon completing the whole-genome sequencing of strain YN1, a comprehensive quality assessment of the sequencing data was performed. The analysis revealed that the genome coverage surpassed 99%, while the contamination rate was below 1%, indicating that the sequencing quality was robust and suitable for subsequent bioinformatics analysis (Figure 2A,B). Subsequent sequence alignment and assembly determined that the genome of strain YN1 comprises a circular chromosome measuring 4,951,512 base pairs (bp) with a GC content of 50.69%, in addition to a circular plasmid of 130,938 bp (Figure 3A,B). Comparative analysis utilizing the PubMLST database classified the core genome multilocus sequence typing (cgMLST) of strain YN1 as cgST134023.

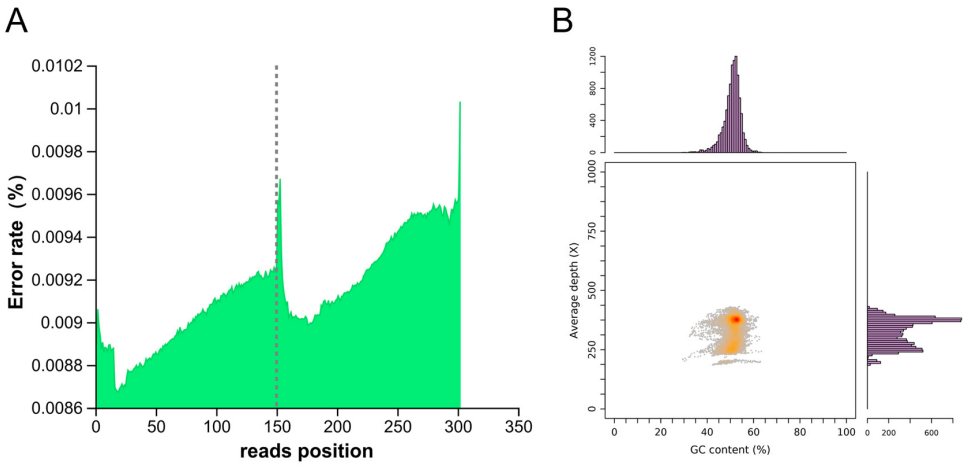

Figure 2. Quality assessment of whole-genome sequencing data for strain YN1. (**A**) Distribution of base error rates across read positions. The x-axis represents the base position within reads, from the 5′ to the 3′ end, and the y-axis represents the average error rate (%) at each position. The first and second halves correspond to reads from the two ends of paired-end sequencing. (**B**) GC content versus sequencing depth. Each point represents a read, with the x-axis indicating GC content and the y-axis indicating sequencing depth; the marginal histograms show the sliding-window frequency distributions of GC content and depth, respectively. A concentrated distribution of points within a narrow range indicates the absence of contamination.

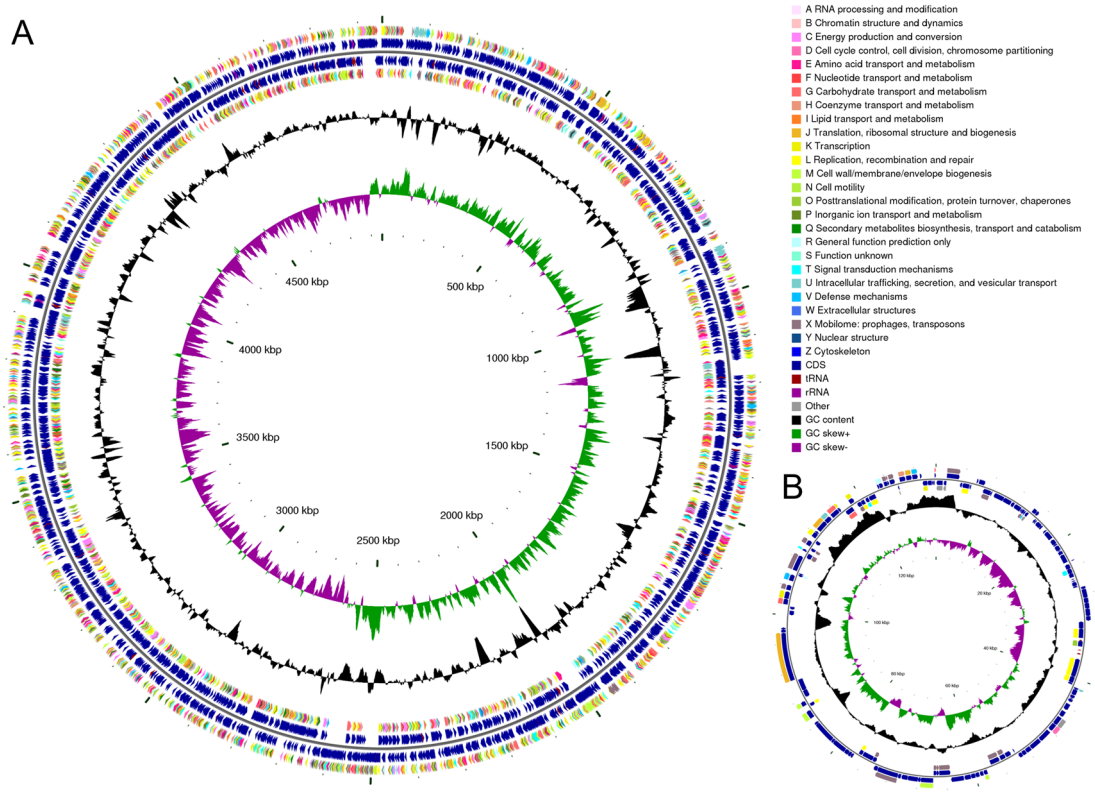

Figure 3. Circular genome maps of strain YN1. (**A**) Chromosome. (**B**) Plasmid. From the outside to the inside, the six concentric circles represent: (i) CDS on the positive strand, (ii) CDS, tRNA, and rRNA on the positive strand, (iii) CDS, tRNA, and rRNA on the negative strand, (iv) CDS on the negative strand, (v) GC content (outward peaks indicate regions above the genome-wide average; inward peaks indicate regions below), and (vi) GC skew (peaks indicate deviation from the average). Different colors in the first and fourth circles denote different COG functional classifications.

3.4. Gene Prediction and Functional Annotation Results

Through alignment with the COG database, a total of 4410 genes were categorized into COG functional categories. Specifically, 1321 genes were associated with cellular processes and signal transduction, 801 genes were linked to information storage and processing, 1874 genes were related to metabolism, and 414 genes were classified as having unknown functions. Within the COG functional categories, the predominant groups comprised genes involved in transcription, cell membrane biosynthesis, metabolism and energy production (Figure 4A). Furthermore, GO analysis results annotated 2204 genes, including 465 genes associated with biological processes, 761 genes related to cellular components, and 978 genes linked to molecular functions. The findings predominantly encompassed the regulation of DNA-templated transcription, cell wall organization, and proteolysis (biological processes); the plasma membrane, cytosol, cytoplasm, and membrane (cellular components); as well as DNA binding, metal ion binding, ATP binding, DNA-binding transcription factor activity, and magnesium ion binding (molecular functions). These results suggest that this strain exhibits robust capabilities in cellular transport, regulation, and energy-dependent processes, aligning with its adaptability and pathogenicity (Figure 4B). KEGG analysis results show that 20 major pathways are involved in various biological processes related to YN1. The top-ranked pathways include metabolic pathways (ko01100), secondary metabolite biosynthesis (ko01110), ABC transporters (ko02010), and microbial metabolic pathways in different environments (ko01120) (Figure 4C).

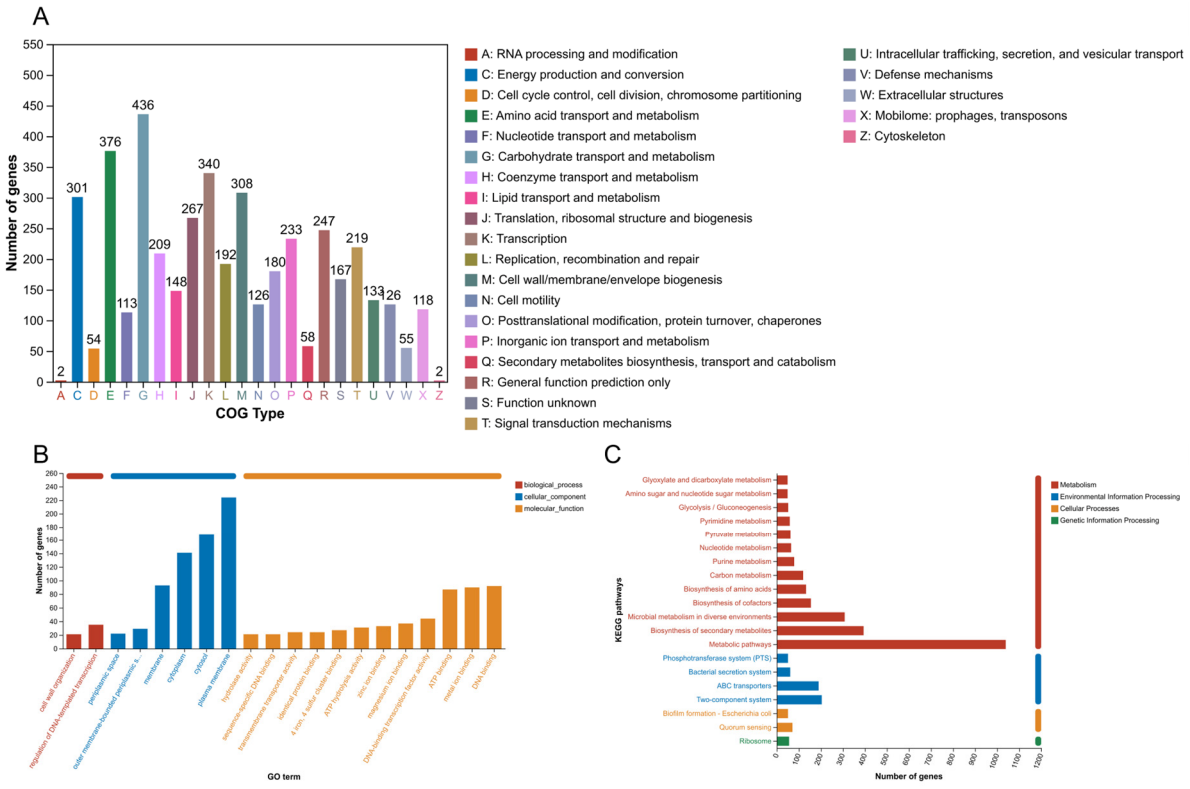

Figure 4. COG, GO, and KEGG functional annotation of the YN1 genome. (**A**) COG classification. The x-axis represents COG functional categories and the y-axis represents the number of genes; the legend on the right defines each COG category. (**B**) GO classification. The x-axis represents the three GO branches—biological process (BP), cellular component (CC), and molecular function (MF)—together with their level-2 subcategories, and the y-axis represents the relative proportion of annotated genes. (**C**) KEGG classification. The y-axis represents level-2 KEGG pathway categories and the x-axis represents the number of genes within each category; colors denote level-1 KEGG categories, and the bar on the far right shows the total number of genes in each level-1 category.

3.5. Results of Antimicrobial Resistance Gene Analysis

The alignment with the CARD identified 863 candidate antibiotic resistance genes (ARGs) in YN1. Following the elimination of duplicate genes and those exhibiting low correlation, 107 primary ARGs were identified, including 101 chromosomally located genes and six plasmid-associated genes. Statistical analysis indicated that ARGs linked to antibiotic efflux were the most prevalent, numbering 64, with 62 situated on chromosomes and 2 on plasmids. Notable efflux pumps include ABC-type, RND-type, and MFS-type, which are associated with resistance to antibiotics such as fluoroquinolones, tetracyclines, and macrolides. Subsequently, ARGs associated with antibiotic target alteration were identified, totaling 22, all of which were chromosomally located. This category of resistance is linked to antibiotics such as peptidoglycan-modifying agents, macrolides, and lincosamides. Furthermore, a total of 11 antibiotic inactivation resistance genes were identified, with 8 located on chromosomes and 3 on plasmids. The expression of these genes is crucial in conferring resistance to aminoglycosides and cephalosporins. The remaining 8 chromosomal resistance genes and 2 plasmid resistance genes were found to reduce the toxicity of antibiotics. Notably, seven of these resistance genes demonstrated multi-drug resistance, simultaneously facilitating diverse mechanisms such as antibiotic efflux, modification of antibiotic binding sites, and decreased antibiotic permeability. (Figure 5A,D).

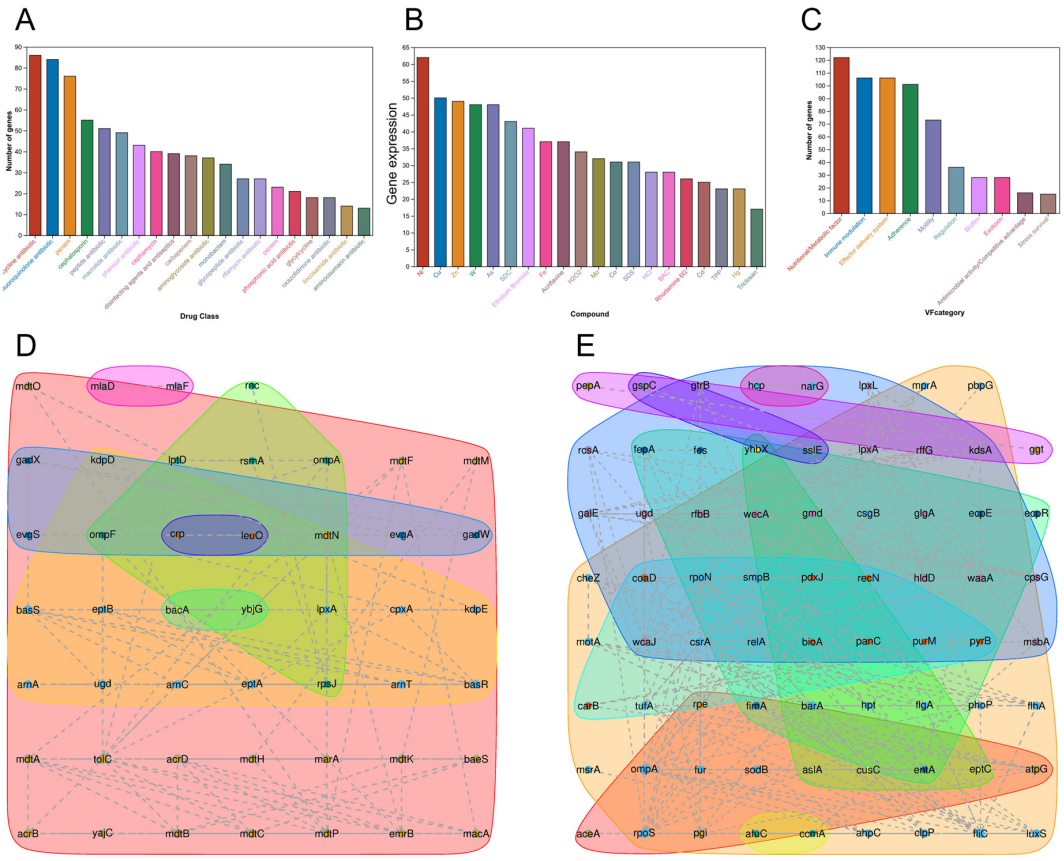

Figure 5. Results of drug resistance and virulence gene analysis. (**A**) Bar chart showing the distribution of predicted drug resistance genes after alignment with the CARD. (**B**) Chart showing the predicted results for metal resistance genes and antimicrobial agents. (**C**) Bar chart showing the distribution of predicted virulence genes after alignment with the VFDB. (The x-axis represents different categories; the y-axis represents the number of genes; different colors correspond to different gene categories.) (**D**) Interaction network diagram for the top-ranked predicted resistance genes. (**E**) Interaction network diagram for the top-ranked predicted virulence genes.

3.6. Results of a Comparison Between Antimicrobial Agents and Metal Resistance Genes

A comparative analysis with the antibacterial biocide and metal resistance genes database identified that strain YN1 harbored 40 distinct types of predicted biocide and metal resistance genes. Notably, the metals exhibiting the highest number of associated resistance genes were nickel, copper, zinc, and arsenic. In terms of biocides, the compounds with the most resistance genes were ethidium bromide, acriflavine, and hydrogen peroxide. The expression of these resistance genes facilitates the strain's enhanced adaptation to the challenging conditions imposed by heavy metals and disinfectants (Figure 5B).

3.7. Results of Virulence Factor Analysis

Alignment with the VFDB revealed that YN1 harbored 653 candidate virulence genes. Following the exclusion of duplicate genes and those with low correlation, 204 major virulence genes were identified, with 203 located on chromosomes and one on a plasmid. Statistical results show that the top-ranked virulence gene clusters include Immune modulation (43), Nutritional/Metabolic factors (37), Effector delivery system (31), Adherence (26), and Biofilm (10). The remaining 57 virulence genes are primarily associated with Motility, Regulation, and Survival under stress. (Supplementary Material—Virulence Gene Details Table). These virulence factors are involved in a variety of biological processes, such as bacterial proliferation, extracellular polysaccharide production, flagellar synthesis, intercellular aggregation, cytotoxicity, biofilm formation, and cellular invasion. (Figure 5C,E).

3.8. Metabolic System Analysis Results

Following a comparative analysis with the Carbohydrate Enzyme Database, a total of 118 genes associated with carbohydrate enzymes were annotated. These included 49 glycosidase genes, 35 glycosyltransferase genes, 22 carbohydrate esterase genes, 10 co-oxidoreductase genes, and 2 carbohydrate-binding module genes (Figure 6A). Furthermore, 40 genes related to secondary metabolites were identified, which are capable of encoding multifunctional enzymes. The investigation of mobile genetic elements within the YN1 strain identified 34 annotated elements, comprising 16 insertion sequences, 12 genomic islands, 4 prophages, one integron, and one plasmid (Same plasmid as above) (Figure 6B).

3.9. PCR Confirmation Results for Key Antimicrobial Resistance and Virulence Genes

The conventional PCR assay successfully amplified the selected key genes from the genomic DNA of strain YN1. Among the antibiotic resistance genes, determinants conferring resistance to β-lactams (e.g., blaTEM), tetracyclines (e.g., tetA), and sulfonamides (e.g., sul2), as well as genes involved in antibiotic efflux (e.g., tolC), were all found to be expressed (Figure 7A,D). Similarly, PCR amplification confirmed the presence of critical virulence genes, including those associated with adhesion, toxin production, and genes located on virulence islands. These results provide evidence that these resistance and virulence genes are indeed present in the genome of YN1, corroborating the WGS predictions (Figure 7E).

3.10. Biofilm Validation Results

After 24 h of incubation across different groups, the removal of the bacterial solution and subsequent staining of the plates revealed a distinctly deep purple ring adhering to the well walls for YN1, in contrast to a pale purple ring observed for the standard strain. Upon dissolution with alcohol, the absorbance at 595 nm (OD = 595) for YN1 was significantly higher than that of the standard strain ($p < 0.01$) (Figure 7B,C).

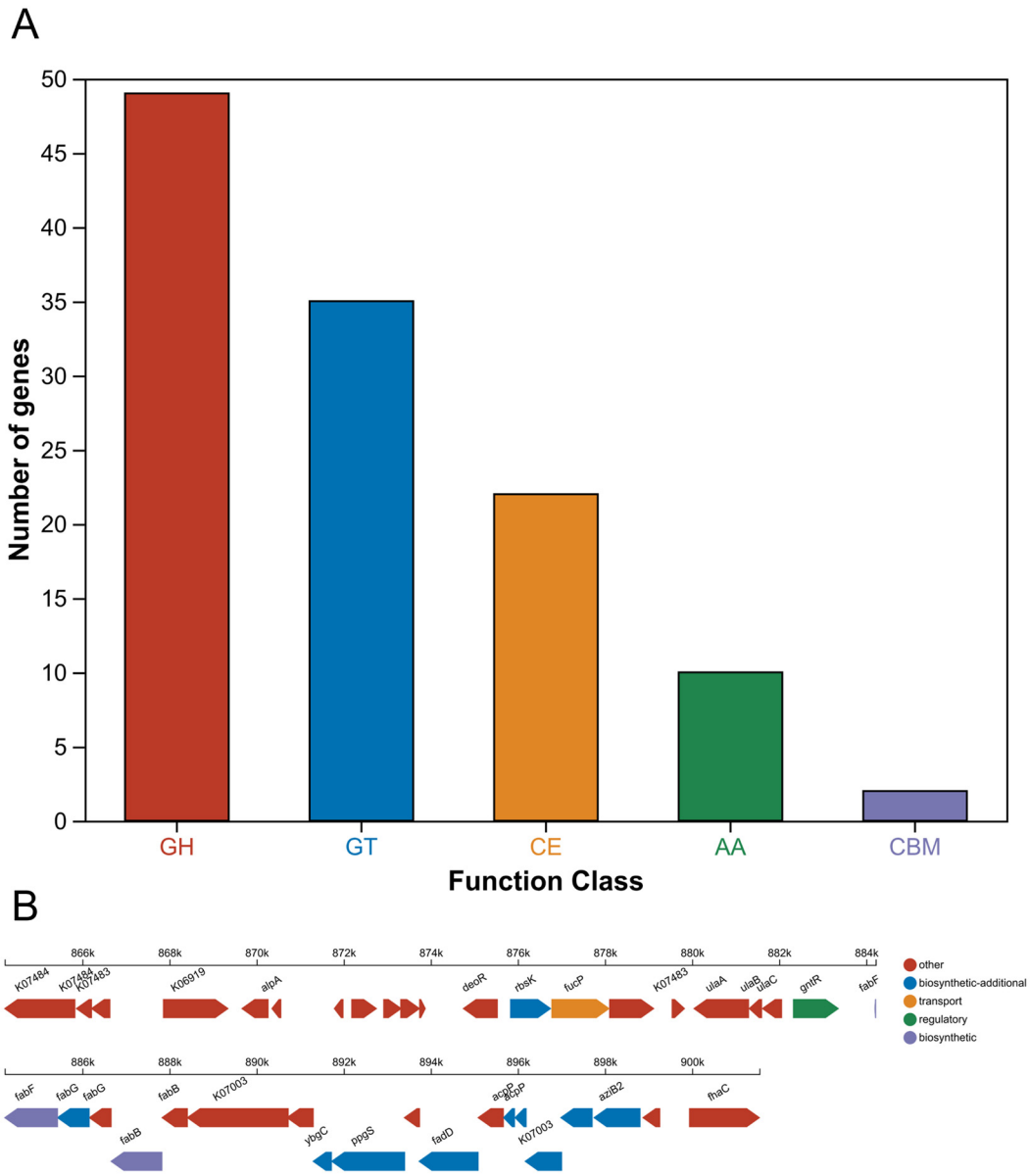

Figure 6. Results of the metabolic system analysis. (**A**) Bar chart showing the distribution of relevant genes after alignment with the Carbohydrate Enzyme Database; the x-axis represents different categories, the y-axis represents the number of genes, and different colors correspond to different classes of carbohydrate-active enzymes. (**B**) Linear diagram of gene clusters involved in secondary metabolite synthesis. The diagram displays all genes in the predicted gene clusters; each arrow represents a gene, with the arrow's length indicating the gene's size and its direction indicating whether the gene is encoded by the forward or reverse strand. Different arrow colors represent the functional classifications of genes within that secondary metabolite synthesis gene cluster.

3.11. Pathogenicity Test Results

Following the intraperitoneal administration of pathogenic bacteria into mice, the mice developed clinical signs, including depression, anorexia, lethargy, ruffled fur, and increased ocular discharge. The animals died after a mean of 16 h. Confirmatory assays identified the isolation of YN1 from the blood and organs of the affected mice. Necropsy findings indicated varying degrees of congestion, stasis, and enlargement in the liver, lungs, and spleen. Pathogenic YN1 was consistently isolated from the blood samples. Histological examination of tissue sections revealed pronounced hemorrhage and stasis within the lungs, spleen, and liver of the experimental group, accompanied by significantly elevated

histological scores ($p < 0.001$). In contrast, all parameters in the control group remained within normal limits (Figure 8A–C).

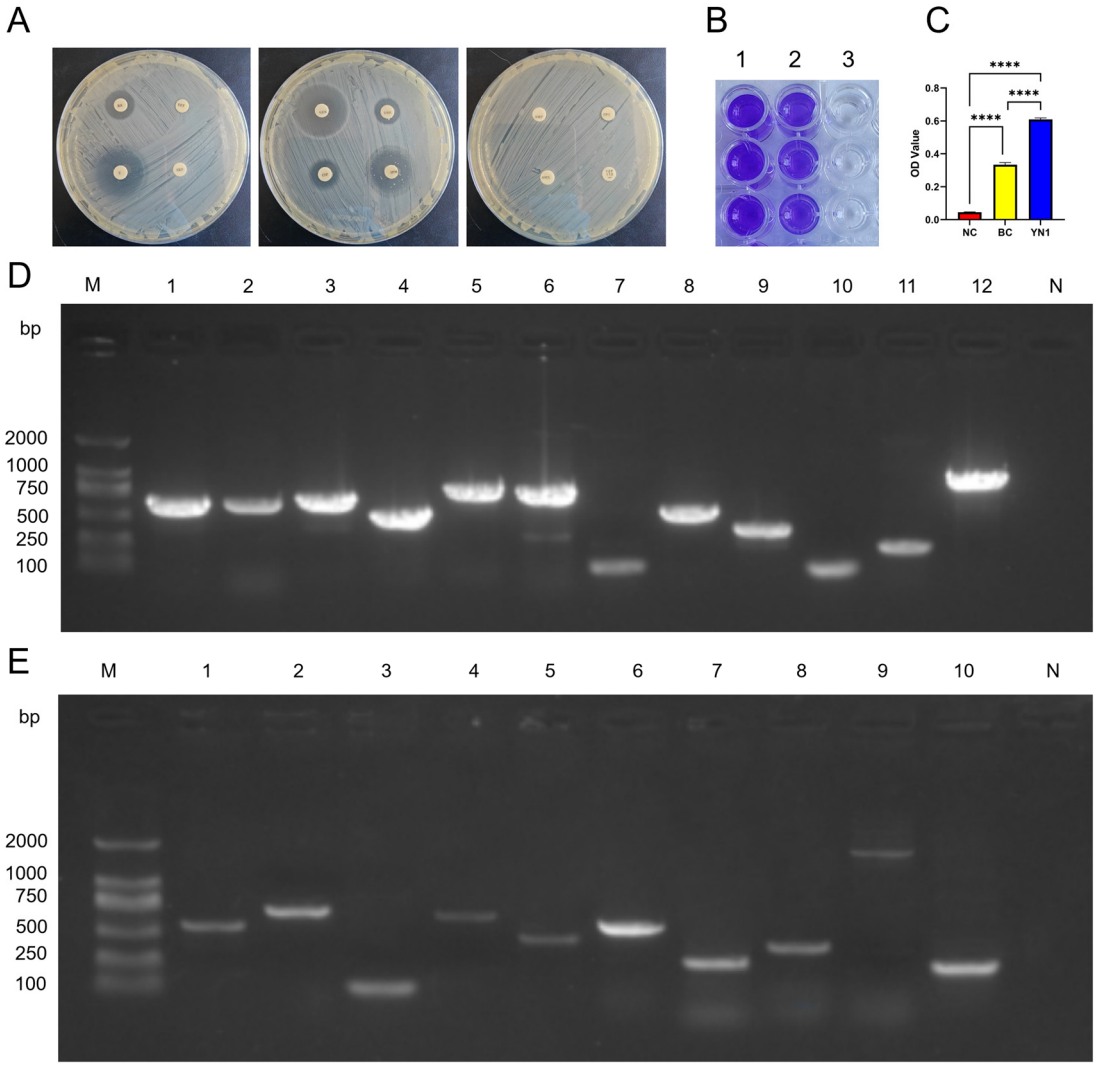

Figure 7. Results of representative antibiotic resistance genes, virulence genes, and biofilm formation assays. (**A**) Antibiotic susceptibility test results. (**B**) Biofilm formation assay results: 1: YN1, 2: reference strain, 3: blank control. (**C**) Statistical results of biofilm OD values; ****: $p < 0.0001$. (**D**) Gel electrophoresis results of PCR products for resistance genes; 1: *sul2*, 2: *blaTEM*, 3: *gyrB*, 4: *gyrA*, 5: *parC*, 6: *tetA*, 7: *sul1*, 8: *floR*, 9: *acrA*, 10: *emrB*, 11: *ant3*, 12: *tolC*, M: Marker, N: Control group. (**E**) Gel electrophoresis results for PCR products of virulence genes; 1: *hlyF*, 2: *fyuA*, 3: *astA*, 4: *sepA*, 5: *fimC*, 6: *iss*, 7: *iutA*, 8: *vat*, 9: *K99*, 10: *rpoS*, M: Marker, N: Control group.

3.12. Results of Sensitivity Drug Therapy

As an exploratory clinical observation, 12 foals with diarrhea were treated with gentamicin. In these cases, the symptoms of diarrhea improved after three days, and the consistency of feces changed from liquid to solid. The whole blood cell count showed that the percentage of red blood cells increased before treatment, indicating dehydration and returning to normal level after treatment (Supplementary Materials-clinical treatment results).

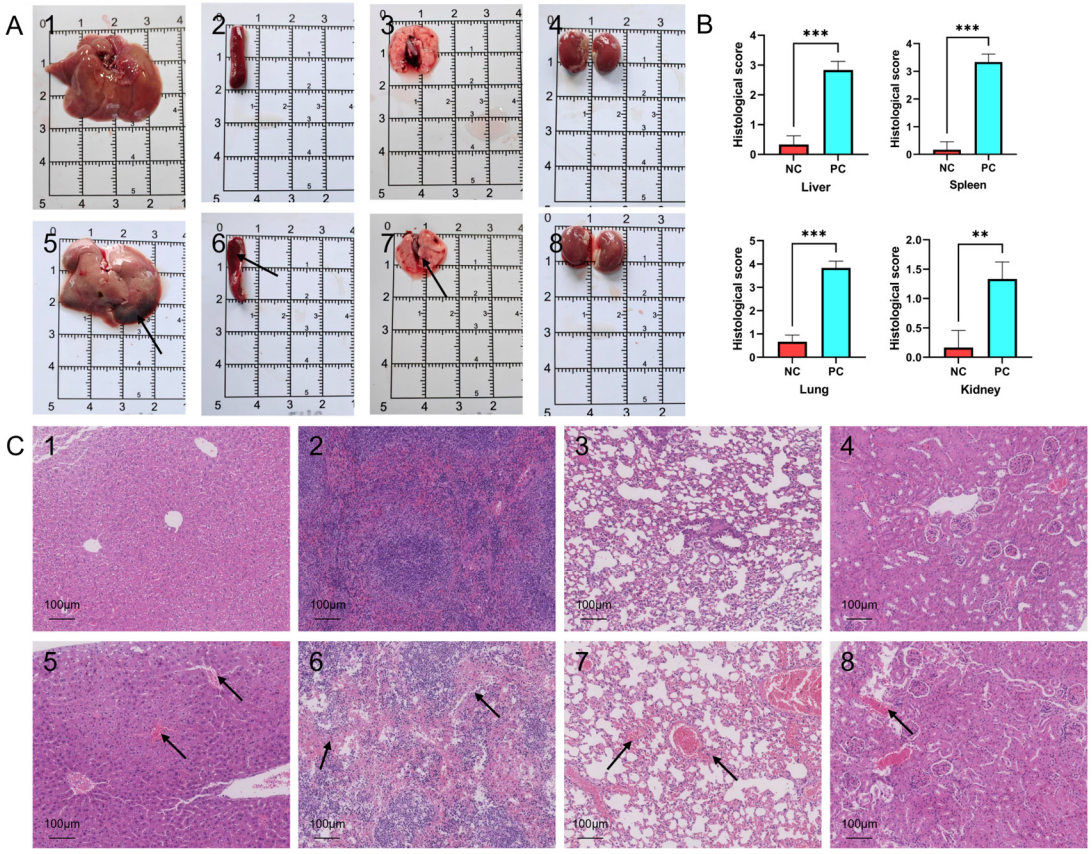

Figure 8. Macroscopic and histopathological findings in infected mice. (**A**) Macroscopic findings; (**1**–**4**): liver, spleen, lung, and kidney from the control group; (**5**–**8**): liver, spleen, lung, and kidney from the experimental group. Arrows indicate obvious hemorrhagic foci and enlargement. (**B**) Bar chart showing histological scoring statistics. **: $p < 0.01$, ***: $p < 0.001$. (**C**) H&E-stained mouse tissue sections; (**1**–**4**): liver, spleen, lung, and kidney from the control group; (**5**–**8**): liver, spleen, lung, and kidney from the pathological group. Arrows indicate: obvious hemorrhagic foci, increased interstitial space, and increased numbers of immune cells.

4. Discussion

The emergence of MDR *E. coli* in agricultural ecosystem marks a key turning point in the global crisis of AMR, and its far-reaching impact is not limited to the veterinary field, but also affects public health and food security [18–20]. Our study of strain YN1, isolated from a diarrheic foal in Ili, Xinjiang, reveals a genome that simultaneously encodes 107 resistance genes and 204 virulence determinants, together with strong biofilm formation and rapid lethality in a murine model. These findings challenge the assumption that horses are merely passive carriers of resistant bacteria and instead position them as active reservoirs capable of accumulating and potentially disseminating clinically significant resistance and virulence traits.

4.1. Interpretation and Mechanistic Analysis

The isolation rate of *E. coli* at 74.36% from diarrheic foals aligns with its established role as a primary enteric pathogen in young livestock. Of particular interest is the age-stratified pattern observed: the isolation rate decreased consistently from 83.33% in foals aged 0–3 months to 53.85% in those aged 6–12 months. This gradient likely reflects the interaction between immature mucosal immunity and the developing gut microbiota in neonates. During the initial weeks of life, the intestinal ecosystem of foals is relatively unstable, characterized by limited colonization resistance and a higher prevalence of op-

portunistic pathogens that can exploit the naive mucosal immune system [21,22]. The predominance of *E. coli* during this period is thus not solely epidemiological but also ecological: the neonatal gut provides a permissive niche where horizontally acquired resistance and virulence factors confer a fitness advantage.

The genomic architecture of YN1 provides a coherent mechanistic explanation for its MDR phenotype. The strain carries 64 efflux pump-associated resistance genes, predominantly of the RND, ABC, and MFS families, which collectively mediate reduced intracellular accumulation of fluoroquinolones, tetracyclines, and macrolides [23,24]. This configuration aligns precisely with the phenotypic resistance profile of the isolate collection. The predominance of efflux-mediated resistance is mechanistically significant: unlike enzymatic inactivation, which imposes a direct fitness cost through protein synthesis and substrate turnover, efflux pumps are frequently chromosomally encoded and tightly regulated, permitting expression to be induced only under antimicrobial pressure [25]. This architecture may explain why YN1 maintains its resistance phenotype without an apparent growth penalty—a prerequisite for successful transmission. The additional presence of 11 antibiotic inactivation genes, including the plasmid-borne *blaTEM*, provides an additional potential mechanism of resistance. The co-occurrence of enzymatic inactivation and efflux-mediated resistance is a hallmark of highly resistant clinical isolates and implies that YN1 has undergone sequential acquisition of resistance determinants under sustained selective pressure [26,27]. The plasmid localization of *blaTEM* is particularly concerning, as it situates a clinically critical β-lactamase gene within a mobilizable genetic context.

Beyond resistance, the genome-wide annotation of YN1 revealed a metabolic and regulatory architecture that further supports its adaptive success. The KEGG analysis results show that the top-ranked pathways primarily include metabolism-related pathways and environment-interaction-related pathways. This enrichment pattern is not incidental: secondary metabolite biosynthesis is frequently linked to the production of siderophores, toxins, and signaling molecules that enhance niche competition and host colonization, while the broad representation of environmental metabolism genes indicates substantial metabolic plasticity. Such plasticity enables the strain to respond to fluctuating nutrient availability and to persist under the selective pressures imposed by antimicrobial exposure. In parallel, the annotation of 118 carbohydrate-active enzymes—including 49 glycosidases, 35 glycosyltransferases, 22 carbohydrate esterases, 10 auxiliary oxidoreductases, and 2 carbohydrate-binding modules—suggests that YN1 is well equipped to degrade and modify host-derived glycans, a capability that may facilitate mucosal colonization and nutrient acquisition within the intestinal environment. Collectively, these metabolic features complement the resistance and virulence repertoires identified in YN1 and provide a more complete picture of the genomic basis of its ecological success.

The virulence repertoire of YN1 reinforces its pathogenic potential. The genome encodes 204 virulence determinants, with the largest subsets associated with immune modulation (43 genes) and nutritional/metabolic factors (37 genes), followed by effector delivery systems, adherence, biofilm formation, regulation, and stress survival. The prominence of immune-modulatory genes is particularly noteworthy, as it suggests that YN1 is capable of actively subverting host innate and adaptive responses—an ability that would favor both intestinal persistence and systemic dissemination. These factors participate in flagellar synthesis, extracellular polysaccharide production, intercellular aggregation, cytotoxicity, and cellular invasion [28–30]. Functionally, YN1 formed significantly stronger biofilms than the reference strain ATCC 25922 ($p < 0.01$), a phenotype that directly enhances antibiotic tolerance by creating a physical barrier and reducing metabolic activity, thereby promoting persister cell formation. Importantly, biofilm formation also facilitates horizontal gene transfer through quorum-sensing-regulated plasmid exchange, further

accelerating the evolution of MDR strains [31]. In the murine infection model, YN1 caused 100% mortality within an average of 16 h, with severe hemorrhage and congestion in the lungs, spleen, and liver, confirming that its virulence gene repertoire translates into genuine pathogenic capacity.

4.2. Comparison with Existing Literature

The MDR rate of 63.79% observed in this study is comparable to, albeit slightly lower than, the 70% reported for equine populations in other regions of Xinjiang [32]. This suggests that MDR *E. coli* is an endemic characteristic of equine populations in this area, rather than a phenomenon limited to localized outbreaks. More broadly, our findings are consistent with previous studies showing that various animal species in Xinjiang can carry ESBL- or pAmpC-producing *E. coli*, and all enterotoxin-induced strains show multiple drug resistance [33]. The STb sequence of the foal isolate clusters phylogenetically with that of a human enterotoxigenic *E. coli* (*ETEC*) strain, which provides evidence of zoonotic potential. Although our study did not conduct a phylogenetic comparison of virulence genes with human isolates, the identification of 204 virulence determinants in the YN1 strain—including genes associated with immune modulation, adherence, and biofilm formation—indicates that this strain possesses the functional repertoire necessary for both intestinal and extraintestinal pathogenesis.

The observed pattern of antimicrobial resistance provides valuable insights when analyzed in conjunction with prescribing practices. Enrofloxacin, doxycycline, and sulfonamide combinations are among the most frequently prescribed oral antimicrobials in equine medicine [34,35]. The relatively high susceptibility rates to enrofloxacin (91.4%) and tetracycline (89.7%) in our sample may initially suggest a lack of direct selective pressure from these agents. Nevertheless, the increased resistance to ampicillin (41.4%, non-susceptible) and amoxicillin (25.9%)—agents infrequently utilized in equine practice—indicates a more intricate selective environment. The presence of β-lactam resistance in the absence of β-lactam usage implies either co-selection via linked resistance determinants or horizontal gene transfer from environmental or human-associated sources. This finding is consistent with the broader understanding that resistance in animal reservoirs cannot be solely attributed to local antimicrobial usage patterns.

4.3. Theoretical and Practical Implications

The findings of this study contribute to the development of a theoretical framework that recognizes equines as underappreciated "bridge hosts" within the ecology of antimicrobial resistance. In contrast to intensively farmed livestock, equines occupy a distinct epidemiological niche: they frequently engage in close contact with humans, yet they are administered antimicrobials less intensively than production animals and are seldom included in systematic resistance surveillance. This unique combination of factors creates a scenario where equines may accumulate resistance determinants from human and environmental sources without experiencing the high antibiotic pressure typical of food animal production. Consequently, equines may serve as a silent reservoir, with their resistance burden becoming apparent only upon clinical infection.

The practical implications for equine medicine and public health are significant. The high prevalence of MDR and genomic evidence indicating transferable resistance determinants in YN1 necessitate the inclusion of equine *E. coli* in regional antimicrobial resistance surveillance programs. The identification of a strain capable of inducing rapid lethality in a murine model highlights that MDR equine *E. coli* represents not merely a colonization issue but a substantial pathogenic threat. Clinically, the sustained susceptibility to gentamicin (100%) and the carbapenem imipenem (82.8%)—the latter being particularly noteworthy

due to its restricted use in veterinary medicine—suggests that treatment options remain, although their continued efficacy cannot be presumed. Consequently, the judicious use of these agents in equine practice, guided by culture and susceptibility testing rather than empirical prescription, is imperative from both clinical and public health perspectives.

4.4. Limitations and Future Directions

Several limitations should be acknowledged. First, whole-genome sequencing was performed on a single representative strain, which cannot capture the genetic diversity of MDR *E. coli* circulating in the Ili equine population; the genomic findings should therefore be regarded as an existence proof rather than a population-level estimate. Second, the sample size (78 fecal samples, 58 isolates) and the restriction to a single region (Ili, Xinjiang) limit the generalizability of our findings to other horse-breeding regions in China. The present data should therefore be interpreted as a regional baseline rather than a nationally representative survey. Third, the conjugative transferability of the *blaTEM* carrying plasmid was not experimentally verified, leaving its mobilization potential speculative. Fourth, the pathogenicity of YN1 was assessed using an intraperitoneal murine infection model, which primarily reflects systemic acute virulence rather than the natural enteric pathogenesis of foal diarrhea. This model does not fully recapitulate the intestinal colonization, mucosal adhesion, or age-dependent susceptibility associated with natural infection in foals, and the results should therefore be interpreted as evidence of pathogenic potential rather than a direct model of the natural disease process. Future research should include multi-regional sampling in Xinjiang and other provinces where horses are raised, expand the scope of genomic testing, and combine cgMLST with plasmid replicon analysis; verify plasmid transferability through conjugation experiments; and integrate longitudinal sampling of foals with metagenomic analysis of the developing gut microbiome. Such work would convert the present descriptive findings into a predictive framework for antimicrobial resistance risk assessment in equine medicine.

5. Conclusions

This study provides phenotypic and genomic insights into multidrug-resistant (MDR) *E. coli* from diarrheic foals in Ili, Xinjiang. The findings indicate that the neonatal equine gut is a permissive niche for these pathogens. Genomic analysis of strain YN1 revealed a sophisticated resistance and virulence architecture, driven by chromosomally encoded efflux systems and supplemented by plasmid-borne β-lactamase genes and mobile genetic elements. This genomic potential translated into strong biofilm formation and severe systemic pathogenicity in vivo. Conceptually, these results position horses as potential "bridge hosts" within the One Health framework, acting as silent reservoirs that accumulate resistance determinants and may facilitate cross-species dissemination. Practically, the high MDR prevalence underscores the urgent need to transition from empirical antimicrobial prescription to culture-guided therapy in equine practice. We therefore advocate for integrating equine E. coli into regional AMR surveillance networks and recommend further multi-regional studies to clarify the broader epidemiological significance of these findings at the human–horse interface.

Supplementary Materials: The following supporting information can be downloaded at: https://www.mdpi.com/article/10.3390/vetsci13111237/s1, Figure S1: Results of 16S sequencing alignment for *E. coli* isolated from normal pony feces; Figure S2: Sensitivity test of YN1 strain to enrofloxacin (double dilution method); Figure S3: Detection of related specific genes of selected strains; Table S1: Results of antimicrobial susceptibility testing for the isolated strains.

Author Contributions: X.D., X.L. and Y.M.: Methodology; X.D., X.L. and T.W.: Software; X.D. and Y.Z.: Formal analysis; X.D. and T.W.: Data curation; X.D., X.L. and H.F.: Writing—original draft; Y.Z. and H.F.: Writing—review & editing; H.F., Y.M. and Y.Z.: Funding acquisition. All authors have read and agreed to the published version of the manuscript.

Funding: This research was supported by the Tianchi Talents Program Grant No: None), the National Natural Science Foundation (Grant No. 32273078), and the Natural Science Fund of Heilongjiang Province (Grant No. ZL2024C020).

Institutional Review Board Statement: This study strictly abides by international animal welfare and ethical standards, and has passed the animal ethics audit of Northeast Agricultural University (ethical code: NEAUEC202603110, date: 15 April 2026).

Informed Consent Statement: Written informed consent has been obtained from the animal owner/data owner to publish this paper.

Data Availability Statement: The data presented in this study are available on request from the corresponding author. The data are not publicly available due to privacy.

Conflicts of Interest: Yuhui Ma is from Xinjiang Zhaosu County Xiyu Horse Industry Co., Ltd., Zhaosu, China. The authors declare that the research was conducted in the absence of any commercial or financial relationships that could be construed as potential conflicts of interest.

References

1. Jee, Y.; Carlson, J.; Rafai, E.; Musonda, K.; Huong, T.T.G.; Daza, P.; Sattayawuthipong, W.; Yoon, T. Antimicrobial resistance: A threat to global health. *Lancet Infect. Dis.* **2018**, *18*, 939–940. [CrossRef]
2. Zambrano, M.M. Interplay between antimicrobial resistance and global environmental change. *Annu. Rev. Genet.* **2023**, *57*, 275–296. [CrossRef]
3. Kabir, A.; Lamichhane, B.; Habib, T.; Adams, A.; El-Sheikh Ali, H.; Slovis, N.M.; Troedsson, M.H.; Helmy, Y.A. Antimicrobial resistance in equines: A growing threat to horse health and beyond—A comprehensive review. *Antibiotics* **2024**, *13*, 713. [CrossRef]
4. Maddox, T.; Clegg, P.; Williams, N.; Pinchbeck, G. Antimicrobial resistance in bacteria from horses: Epidemiology of antimicrobial resistance. *Equine Vet. J.* **2015**, *47*, 756–765. [CrossRef]
5. Tyrnenopoulou, P.; Tsilipounidaki, K.; Florou, Z.; Gkountinoudis, C.-G.; Tyropoli, K.; Starras, A.; Peleki, C.; Marneris, D.; Arseniou, N.; Lianou, D.T. Detection of Gastrointestinal Pathogens with Zoonotic Potential in Horses Used in Free-Riding Activities during a Countrywide Study in Greece. *Animals* **2024**, *14*, 2566. [CrossRef]
6. Reshadi, P.; Heydari, F.; Ghanbarpour, R.; Bagheri, M.; Jajarmi, M.; Amiri, M.; Alizade, H.; Badouei, M.A.; Sahraei, S.; Adib, N. Molecular characterization and antimicrobial resistance of potentially human-pathogenic *Escherichia coli* strains isolated from riding horses. *BMC Vet. Res.* **2021**, *17*, 131. [CrossRef]
7. Van Spijk, J.; Schmitt, S.; Schoster, A. Infections caused by multidrug-resistant bacteria in an equine hospital (2012–2015). *Equine Vet. Educ.* **2019**, *31*, 653–658. [CrossRef]
8. Shoaib, M.; Gul, S.; Majeed, S.; He, Z.; Hao, B.; Tang, M.; Zhang, X.; Wu, Z.; Wang, S.; Pu, W. Pathogenomic Characterization of Multidrug-Resistant *Escherichia coli* Strains Carrying Wide Efflux-Associated and Virulence Genes from the Dairy Farm Environment in Xinjiang, China. *Antibiotics* **2025**, *14*, 511. [CrossRef]
9. Ding, X.; An, Q.; Kang, H.; Li, S.; Zhang, S.; Yang, H.; Dou, X.; Ji, Y.; Zhao, Y.; Fan, H. Whole-Genome Analysis of a Novel Multidrug-Resistant *Escherichia coli* Strain from Dairy Calves in Northeast China: Mechanisms of Antibiotic Resistance and Biofilm Formation. *Biology* **2025**, *14*, 1257. [CrossRef]
10. Punina, N.; Makridakis, N.; Remnev, M.; Topunov, A. Whole-genome sequencing targets drug-resistant bacterial infections. *Hum. Genom.* **2015**, *9*, 9. [CrossRef]
11. Yang, X.; Wu, T.; Liu, X.; Lv, D.; Zhang, G.; Zhang, S.; Yang, H.; Jiao, W.; Zhao, Y.; Fan, H.; et al. Multidrug-Resistant *Escherichia coli* Antagonized by Luteolin: A Mechanistic Insight into Virulence Suppression and Gut Microbiota Restoration. *Microorganisms* **2026**, *14*, 427. [CrossRef]
12. Humphries, R.; Bobenchik, A.M.; Hindler, J.A.; Schuetz, A.N. Overview of changes to the clinical and laboratory standards institute performance standards for antimicrobial susceptibility testing, M100. *J. Clin. Microbiol.* **2021**, *59*, e0021321. [CrossRef]
13. Alcock, B.P.; Raphenya, A.R.; Lau, T.T.; Tsang, K.K.; Bouchard, M.; Edalatmand, A.; Huynh, W.; Nguyen, A.-L.V.; Cheng, A.A.; Liu, S. CARD 2020: Antibiotic resistome surveillance with the comprehensive antibiotic resistance database. *Nucleic Acids Res.* **2020**, *48*, D517–D525. [CrossRef]

14. Liu, B.; Zheng, D.; Zhou, S.; Chen, L.; Yang, J. VFDB 2022: A general classification scheme for bacterial virulence factors. *Nucleic Acids Res.* **2022**, *50*, D912–D917. [CrossRef]
15. Lombard, V.; Golaconda Ramulu, H.; Drula, E.; Coutinho, P.M.; Henrissat, B. The carbohydrate-active enzymes database (CAZy) in 2013. *Nucleic Acids Res.* **2014**, *42*, D490–D495. [CrossRef]
16. Meroni, G.; Soares Filipe, J.F.; Drago, L.; Martino, P.A. Investigation on antibiotic-resistance, biofilm formation and virulence factors in multi drug resistant and non multi drug resistant *Staphylococcus pseudintermedius*. *Microorganisms* **2019**, *7*, 702. [CrossRef]
17. Ding, X.; Zhao, Y.; Li, J.; Zhang, S.; Yao, D.; Yang, H.; Zhang, Y.; Fan, H. Mechanisms of Inhibitory and Anti-Inflammatory Effects of Aloe-Emodin Against Multidrug-Resistant *Escherichia coli*: A Network Pharmacology and Molecular Dynamics Approach. *J. Food Biochem.* **2025**, *2025*, 5709147. [CrossRef]
18. Chang, Q.; Wang, W.; Regev-Yochay, G.; Lipsitch, M.; Hanage, W.P. Antibiotics in agriculture and the risk to human health: How worried should we be? *Evol. Appl.* **2015**, *8*, 240–247. [CrossRef]
19. Barathe, P.; Kaur, K.; Reddy, S.; Shriram, V.; Kumar, V. Antibiotic pollution and associated antimicrobial resistance in the environment. *J. Hazard. Mater. Lett.* **2024**, *5*, 100105. [CrossRef]
20. Okaiyeto, S.A.; Sutar, P.P.; Chen, C.; Ni, J.-B.; Wang, J.; Mujumdar, A.S.; Zhang, J.-S.; Xu, M.-Q.; Fang, X.-M.; Zhang, C. Antibiotic resistant bacteria in food systems: Current status, resistance mechanisms, and mitigation strategies. *Agric. Commun.* **2024**, *2*, 100027. [CrossRef]
21. Li, Y.; Lan, Y.; Zhang, S.; Wang, X. Comparative Analysis of Gut Microbiota Between Healthy and Diarrheic Horses. *Front. Vet. Sci.* **2022**, *9*, 882423. [CrossRef]
22. Lübke-Becker, D.A.; Krenz, D.M.; van der Grinten, D.E. Enteritis and septicemia in a horse associated with infection by *Escherichia fergusonii*. *J. Equine Vet. Sci.* **2011**, *31*, 361–364. [CrossRef]
23. Bleuel, C.; Große, C.; Taudte, N.; Scherer, J.; Wesenberg, D.; Krauß, G.J.; Nies, D.H.; Grass, G. TolC is involved in enterobactin efflux across the outer membrane of *Escherichia coli*. *J. Bacteriol.* **2005**, *187*, 6701–6707. [CrossRef]
24. Kumawat, M.; Nabi, B.; Daswani, M.; Viquar, I.; Pal, N.; Sharma, P.; Tiwari, S.; Sarma, D.K.; Shubham, S.; Kumar, M. Role of bacterial efflux pump proteins in antibiotic resistance across microbial species. *Microb. Pathog.* **2023**, *181*, 106182. [CrossRef]
25. Novelli, M.; Bolla, J.-M. RND efflux pump induction: A crucial network unveiling adaptive antibiotic resistance mechanisms of gram-negative bacteria. *Antibiotics* **2024**, *13*, 501. [CrossRef]
26. Ansharieta, R.; Ramandinianto, S.C.; Effendi, M.H.; Plumeriastuti, H. Molecular identification of bla CTX-M and bla TEM genes encoding extended-spectrum ß-lactamase (ESBL) producing *Escherichia coli* isolated from raw cow's milk in East Java, Indonesia. *Biodiversitas J. Biol. Divers.* **2021**, *22*, 1600. [CrossRef]
27. Aklilu, E.; Harun, A.; Singh, K.K.B. Molecular characterization of bla NDM, bla OXA-48, mcr-1 and bla TEM-52 positive and concurrently carbapenem and colistin resistant and extended spectrum beta-lactamase producing *Escherichia coli* in chicken in Malaysia. *BMC Vet. Res.* **2022**, *18*, 190. [CrossRef]
28. Pakbin, B.; Brück, W.M.; Rossen, J.W. Virulence factors of enteric pathogenic *Escherichia coli*: A review. *Int. J. Mol. Sci.* **2021**, *22*, 9922. [CrossRef]
29. Haiko, J.; Westerlund-Wikström, B. The role of the bacterial flagellum in adhesion and virulence. *Biology* **2013**, *2*, 1242–1267. [CrossRef]
30. Lian, S.; Luo, Y.; Chen, Z.; Wei, X.; Liu, J.; Zhu, G.; Xia, P. Deficiency of the flagellin subunit FliC exacerbates the pathogenicity of extraintestinal pathogenic *Escherichia coli* in BALB/c mice by inducing a more intense inflammation. *Int. J. Biol. Macromol.* **2025**, *289*, 138761. [CrossRef]
31. Mirghani, R.; Saba, T.; Khaliq, H.; Mitchell, J.; Do, L.; Chambi, L.; Diaz, K.; Kennedy, T.; Alkassab, K.; Huynh, T. Biofilms: Formation, drug resistance and alternatives to conventional approaches. *AIMS Microbiol.* **2022**, *8*, 239. [CrossRef]
32. Liu, H.; Zhu, B.; Qiu, S.; Xia, Y.; Liang, B.; Yang, C.; Dong, N.; Li, Y.; Xiang, Y.; Wang, S. Dominant serotype distribution and antimicrobial resistance profile of *Shigella* spp. in Xinjiang, China. *PLoS ONE* **2018**, *13*, e0195259. [CrossRef]
33. Yang, B.; Xing, G.; Ma, W.; Qi, M.; Jing, B.; Li, J.; Wu, J. Co-existence of blaCTX-M and mcr-1 in avian pathogenic *Escherichia coli* in Southern Xinjiang: Current status and antimicrobial resistance characteristics. *Folia Microbiol.* **2026**, *71*, 1–13. [CrossRef]
34. Barr, B.; Waldridge, B.; Morresey, P.; Reed, S.; Clark, C.; Belgrave, R.; Donecker, J.; Weigel, D. Antimicrobial-associated diarrhoea in three equine referral practices. *Equine Vet. J.* **2013**, *45*, 154–158. [CrossRef]
35. Yang, B.; Liu, S.; Cheng, J.; Qu, H.; Guo, Y.; Ji, C.; Wang, Y.; Zhao, S.; Huang, S.; Zhao, L. Pharmacokinetics of enrofloxacin in plasma, urine, and feces of donkey (equus asinus) after a single intragastric administration. *Antibiotics* **2024**, *13*, 355. [CrossRef]

Disclaimer/Publisher's Note: The statements, opinions and data contained in all publications are solely those of the individual author(s) and contributor(s) and not of MDPI and/or the editor(s). MDPI and/or the editor(s) disclaim responsibility for any injury to people or property resulting from any ideas, methods, instructions or products referred to in the content.